Journal of High Energy Astrophysics 25 (2020) 23–28

Contents lists available at ScienceDirect

Journal of High Energy Astrophysics

www.elsevier.com/locate/jheap

Toward a robust inference method for the likelihood of low-luminosity gamma-ray bursts to be progenitors of ultrahigh-energy cosmic rays correlating with starburst galaxies

Luis A. Anchordoqui [a,b,c,*], Claire Mechmann [a,c], Jorge F. Soriano [a,b]

[a] Department of Physics and Astronomy, Lehman College, City University of New York, NY 10468, USA
[b] Department of Physics, Graduate Center, City University of New York, NY 10016, USA
[c] Department of Astrophysics, American Museum of Natural History, NY 10024, USA

ARTICLE INFO

Article history:
Received 13 December 2019
Received in revised form 27 December 2019
Accepted 13 January 2020

ABSTRACT

Very recently, the Pierre Auger Collaboration reported a 4.5σ correlation between the arrival directions of the highest energy cosmic rays and nearby starburst galaxies. The cosmic rays producing the anisotropy signal have been proposed to originate in low-luminosity gamma-ray bursts (llGRBs). On the basis of the well-justified assumption that at redshift $z < 0.3$ the host metallicity is a good indicator of the llGRB production rate, we show that the association of llGRBs and the starbursts correlating with Auger data is excluded at the 90% confidence level.

1. General idea

By now, it is well-established that galactic-scale outflows of gas (generally called *starburst-driven superwinds*) are ubiquitous in galaxies in which the global star-formation rate per unit area exceeds roughly $10^{-1}\ M_\odot\ \text{yr}^{-1}\,\text{kpc}^{-2}$ (Heckman, 2001). These flows are complex, multiphase phenomena powered primarily by massive star winds and by core collapse supernovae (SNe), which collectively create hot ($T \lesssim 10^8$ K) bubbles of metal-enriched plasma within the star forming regions. The over-pressured bubbles expand at high-velocity sweeping up cooler ambient gas and eventually blow out of the disk into the halo. Starburst superwinds then provide a commonplace for the formation of collisionless plasma shock waves in which charged particles can be accelerated by bouncing back and forth across the shock up to ultrahigh energies (Anchordoqui et al., 1999). Experimental data support this prediction: the Pierre Auger Collaboration reported a 4.5σ significance correlation between the arrival direction of cosmic rays with energy above 38 EeV and a model based on a catalog of bright starburst galaxies (Aab et al., 2018, 2019). In the best-fit model, $11^{+5}_{-4}\%$ of the cosmic-ray flux originates from these objects and undergoes angular diffusion on a scale $\vartheta \sim 15^{+5^\circ}_{-4}$. The latter angular spread derives from a Fisher-Von Mises distribution, the equivalent of a Gaussian on the sphere, and would correspond to a top-hat scale $\varphi \sim 1.59 \times \vartheta$. Of course, readjustment of superwind-free-parameters are necessary to accommodate Auger data (Anchordoqui, 2018, 2019; Anchordoqui and Soriano, 2019).

However, it was recently put forward the idea that ultrahigh-energy-cosmic-ray (UHECR) acceleration in low-luminosity gamma-ray bursts (llGRB) could be the origin of the fraction of Auger events which correlates with starburst galaxies (Zhang et al., 2018). In this work we show that the association of llGRBs with the starbursts generating the anisotropy signal found in Auger data is disfavored by observation. Before proceeding, we pause to note that whether llGRBs would satisfy the power requirements to accelerate cosmic rays up to the highest observed energies may be up for debate (Samuelsson et al., 2019; Zhang and Murase, 2018; Boncioli et al., 2019).

The layout of the paper is as follows: in Sec. 2 we discuss the sample of llGRBs and starburst galaxies we have selected to study and conduct the statistical analysis; in Sec. 3 we draw our conclusions.

2. Data analysis

We begin our study with an overview of the basic properties of the various GRB populations. A detailed scrutiny of the BATSE catalog led to our current duration-based classification system for GRBs: short GRBs (SGRBs) have burst durations of < 2 s, whereas long GRBs (LGRBs) have burst durations of > 2 s (Kouveliotou et al., 1993). GRBs can also be splitted according to their luminosities into llGRBs ($L_{\text{iso}} < 10^{49}$ erg/s) and high-luminosity GRBs ($L_{\text{iso}} > 10^{49}$ erg/s) (Liang et al., 2007). Herein, we also adopt the

* Corresponding author.
E-mail address: luis.anchordoqui@gmail.com (L.A. Anchordoqui).

https://doi.org/10.1016/j.jheap.2020.01.001
2214-4048/

Table 1
Properties of nearby llGRBs.

GRB ID	$\log[L_{\rm iso}/({\rm erg/s})]$	Redshift	$12 + \log({\rm O/H})$	References
980425	46.67	0.008	8.3	(Stanek et al., 2006; Levesque et al., 2010; Virgili et al., 2009)
020903	48.92	0.251	8.0	(Levesque et al., 2010; Virgili et al., 2009; Thöne et al., 2019)
031203	48.55	0.105	8.1	(Levesque et al., 2010; Virgili et al., 2009; Thöne et al., 2019)
051109B	48.22	0.080	···	(Pescalli et al., 2015)
060218	46.78	0.033	8.1	(Levesque et al., 2010; Virgili et al., 2009; Thöne et al., 2019)
060505	48.85	0.089	8.4	(Pescalli et al., 2015; Thöne et al., 2008)
080517	48.52	0.089	8.6	(Li, 2017; Niino et al., 2017; Stanway et al., 2015; Chrimes et al., 2018)
100316D	47.75	0.059	8.2	(Levesque et al., 2011; Dereli et al., 2017; Thöne et al., 2019)
111005A	46.78	0.013	8.6	(Li, 2017; Tanga et al., 2018; Michalowski et al., 2018)
171205A	47.50	0.037	8.4	(Izzo et al., 2019)[a]

[a] An estimate of the GRB 171205A host metallicity is given in the journal (but not in the arXiv) version of (Izzo et al., 2019).

conventions of (Levesque et al., 2010) to identify nearby ($z < 0.3$) GRBs from those at intermediate redshift ($0.3 < z < 1$). We note, however, that recent studies do not show a strong evidence suggesting that $z < 0.3$ GRBs would be, as a population, different from the high-redshift one. Nevertheless, although one can find many high-luminosity GRBs at $z < 0.3$, the llGRBs at $z > 0.3$ cannot be detected due to the sensitivity of the gamma-ray detectors; see e.g. Fig. 1 in (Perley et al., 2014). This last argument further justifies our redshift selection criterion.

Over the last two decades a consensus formed that LGRBs are a product of a core-collapse of a massive star (MacFadyen and Woosley, 1999) and that SGRBs have a different origin. Indeed, observations have proved the SNe type Ic-BL $\leftrightharpoons$ LGRBs connection beyond any reasonable (Woosley and Bloom, 2006; Modjaz et al., 2016; Cano et al., 2017). Type Ic are core-collapse stripped-envelope are core-collapse stripped-envelope SNe, whose progenitor stars have lost most of the hydrogen and helium in their outer envelopes prior to the collapse. Some SNe type Ic are found to have very broad lines in their spectra (type Ic-BL), indicative of very fast ejecta velocities.

Because GRBs are outlying and arise in small galaxies seldom monitored by high-angular resolution surveys, it has not been and will likely not be possible in the near future to image the progenitor of a GRB, thus we are only able to figure out properties of the progenitor star from its environment. There are several studies that seem to indicate that GRB formation efficiency drops at high metallicity. For example, the host galaxies of five nearby LGRBs (980425, 020903, 030329, 031203 and 060218, each of which had a well-documented associated SN) are all faint and metal-poor compared to the population of local star-forming galaxies (Stanek et al., 2006). Moreover, various analyses of GRB host morphologies suggest a correlation between metallicity and LGRB occurrence rate; see e.g. (Kocevski et al., 2009; Trenti et al., 2015). In addition, a systematic comparison of the host galaxies of broad-lined SNe Ic with and without a detected GRB, indicates that a larger fraction of super-solar metallicity hosts are found among the SNe Ic-BL without a GRB (Japelj et al., 2018).

Models of stellar evolution further reinforce the metallicity bias for LGRB progenitors. This is because the well-established correlation between LGRB and stripped-envelope SNe points to carbon- and oxygen- rich Wolf-Rayet (WR) stars as the most promising progenitor candidates (Woosley and Heger, 2006; Langer and Norman, 2006).[1] WR stars emit winds that eject about $10 M_\odot$ of material per million years at speeds of up to 3,000 km/s, resulting in the characteristic broad emission lines in the spectra of these stars (normal stars have narrow emission lines). It is thought that these powerful winds are driven by intense radiation pressure on spectral lines, yielding a dependence of the wind-driven mass loss rate on surface metallicity (Kudritzki, 2002; Vink and de Koter, 2005). Thereupon, the surface rotation velocities of WR stars are expected to decrease at higher stellar metallicities because of the higher mass loss rate (Kudritzki and Puls, 2000). For WR stars, the metallicities characterizing their host environments can be adopted as the natal metallicities of the stars themselves. This entails that the higher wind-driven mass loss rates in metal-rich environments would remove from the massive WR stars too much angular momentum, inhibiting them from rotating rapidly enough to produce a LGRB (Woosley and Heger, 2006; Yoon et al., 2012). All in all, the data seem to indicate that LGRBs should be confined to low-metallicity environments.

Though *a priori* there is no reason to assume that LGRBs and llGRBs are related, the similarity of their associated SNe implies that llGRBs and LGRBs have similar progenitors and similar inner explosion mechanism (Nakar, 2015). In light of the preceding discussion, it seems reasonable to assume that the metallicity of the host environment would also be a good discriminator of llGRB progenitors. In what follows we compare the host metallicity of nearby llGRBs with that of the starbursts dominating the signal in Auger data.

Before we can conduct the statistical analysis, we need to define our samples. The Auger anisotropy search included a sample of 23 starburst galaxies with a flux larger than 0.3 Jy selected out of the 63 objects within 250 Mpc search for γ-ray emission by the Fermi-LAT Collaboration (Ackermann et al., 2012). This selection was updated in (Aab et al., 2019) with the addition of the Circinus Galaxy and sources selected from the HEASARC Radio Master Catalog.[2] The number of starbursts selected this way is 32. Here we consider 10 of these galaxies (including all sources dominating the Auger anisotropy signal) for which the average metallicity has been determined. It is important to note that some galaxies in the starburst sample have a double starburst/AGN nature (e.g., Circinus, NGC 4945, NGC 1068). Given that so far, despite efforts, no GRB host galaxy has been found to host an AGN, it may not come as surprising if the two samples are not drawn from the same underlying probability distribution. We consider all llGRB detected at $z < 0.3$. The metallicities of llGRB hosts are given in Table 1 and the metallicities of the starbursts are given in Table 2. Following (Moreno-Raya et al., 2016), we have taken $\log(Z/Z_\odot) = \log({\rm O/H}) - \log({\rm O/H})_\odot$, with $12 + \log({\rm O/H})_\odot = 8.69$ and $Z_\odot = 0.019$ being the solar values (Asplund et al., 2009).[3]

Before proceeding, some technical remarks are in oder to clarify our metallicity selection criteria. Molecular gas in starbursts exists under conditions very different from those found in most normal galaxies. Observations of starbursts suggest widespread gas volume and column densities much higher than those typical of normal

[1] WR stars are highly luminous massive objects which are at an advanced stage of stellar evolution and losing mass at a very high rate.

[2] https://heasarc.nasa.gov/W3Browse/master-catalog/radio.html.

[3] We note that the precision of our phenomenological study is insensitive to any plausible change of the solar metallicity, e.g., $12 + \log({\rm O/H})_\odot = 8.66$ (Asplund et al., 2004).

Table 2
Properties of nearby starburst galaxies.

Starburst ID	Distance (Mpc)	12+ log(O/H)	References
NGC 253	2.7	8.7	(Aab et al., 2018; Zaritsky et al., 1994; Pilyugin et al., 2004)
M82	3.6	8.8	(Aab et al., 2018; Moreno-Raya et al., 2016)[a]
NGC 4945	4.0	8.5	(Aab et al., 2018; Stanghellini et al., 2015)
M83	4.0	8.8	(Aab et al., 2018; Zaritsky et al., 1994; Pilyugin et al., 2004)
IC 342	4.0	8.8	(Aab et al., 2018; Pilyugin et al., 2004; Hung, 2015)
Circinus	4.0	8.4	(Oliva et al., 1999)[b]
NGC 6946	5.9	8.8	(Aab et al., 2018; Zaritsky et al., 1994; Pilyugin et al., 2004)
M51	10.3	8.8	(Aab et al., 2018; Zaritsky et al., 1994; Pilyugin et al., 2004)
NGC 891	11.0	8.7	(Aab et al., 2018; Galliano et al., 2008; Otte et al., 2001)
NGC 1068	17.9	8.8	(Aab et al., 2018; Zaritsky et al., 1994; Pilyugin et al., 2004)

[a] See, in particular, Table A.1 of (Moreno-Raya et al., 2016).
[b] See, in particular, Table 1 of (Oliva et al., 1999).

disks (Jackson et al., 1995; Paglione et al., 1997). The nebular oxygen abundance is the canonical choice of metallicity indicator for studies of the interstellar medium since oxygen is the most abundant metal, only weakly depleted, and exhibits very strong nebular emission lines in the optical wavelength range (Tremonti et al., 2004). Extensive analyses have been carried out to calibrate metallicity studies by using only strong emission lines. One of the most frequently used metallicity diagnostics is the parameter

$$R_{23} = \log_{10}\{([\text{O}\,\textsc{ii}]\lambda3727 + [\text{O}\,\textsc{iii}]\lambda\lambda4959, 5007)/\text{H}\beta\}\,, \qquad (1)$$

defined as the ratio of the flux in the strong optical oxygen lines to that of Hλ4861 (Pagel et al., 1979); notation conventions are those in (Tendulkar et al., 2017). However, a well-known problem of this metallicity diagnostic is that the R_{23} vs. $12 + \log(\text{O/H})$ relation is double-valued, and so additional information is required to break this degeneracy. Several methods have been developed to remove the R_{23} degeneracy exploiting the [Nɪɪ], [Sɪɪ], and Hα lines; e.g.,

$$\begin{aligned} N2 &= \log_{10}\{[\text{N}\,\textsc{ii}]\lambda6584/\text{H}\alpha\}\,, \\ O3N2 &= \log_{10}\{([\text{O}\,\textsc{iii}]\lambda5007/[\text{N}\,\textsc{ii}]\lambda6584) \times (\text{H}\alpha/\text{H}\beta)\}\,, \\ y &= \log_{10}\{[\text{N}\,\textsc{ii}]\lambda6584/[\text{S}\,\textsc{ii}]\lambda\lambda6717, 6731\} \\ &\quad + 0.264\log_{10}\{[\text{N}\,\textsc{ii}]\lambda6584/\text{H}\alpha\}\,, \end{aligned} \qquad (2)$$

proposed in (Kewley and Dopita, 2002), (Pettini and Pagel, 2004), and (Dopita et al., 2016). Although an absolute calibration for metallicities obtained through the strong-line methods remains uncertain (Kewley and Ellison, 2008), we may still use the strong-line ratios to study the trend in metallicities between the llGRB hosts and starburst galaxies in our sample. Indeed, the absolute metallicity scale varies up to $\Delta[\log(\text{O/H})] = 0.7$, depending on the calibration used, and the change in shape is substantial. It is critical then to use the same metallicity calibration when comparing different metallicity relations. Herein we adopt the $O3N2$ diagnostic with normalization as given in (Pettini and Pagel, 2004),

$$12 + \log(\text{O/H}) = 8.73 - 0.32 \times O3N2\,, \qquad (3)$$

and use the metallicity conversions given in (Kewley and Ellison, 2008), which allow metallicities that have been derived using different strong-line calibrations to be converted to the same base calibration. In Tables 1 and 2 we provide the best-fit values of the metallicities after conversion to the same base calibration. Following (Galliano et al., 2008), an uncertainty of 0.1 dex in the O/H number abundance accounts for the typical dispersion between independent measurements. To remain conservative, in our calculations we adopt the upper and lower end of the 1σ metallicity range to characterize the llGRB and starburst samples, respectively. Concerning GRB 051109B, it has been tentatively associated with a star-forming region in a spiral galaxy which lacks of any strong emission features (Perley et al., 2006). Therefore, we do not include this event in our statistical analysis.

Next, we adopt the Kolmogorov-Smirnov (two-sample) test to check whether the two data sets of metallicity are both drawn from the same underlying probability distribution, but without assuming any specific model for that distribution (Kolmogorov, 1933; Smirnov, 1933). The calculations that are involved in application of the Kolmogorov-Smirnov test are quite simple. We begin by stating the null hypothesis $\mathcal{H}_0$: if $f_m(x)$ and $g_m(x)$ are samples of two underlying probability density functions $f(x)$ and $g(x)$, then

$$\mathcal{H}_0:\ f(x) = g(x)\,, \forall x\,. \qquad (4)$$

The alternate hypothesis is that $f(x) \neq g(x)$. Now, given any sample from an unspecified population, a natural estimate of the unknown cumulative distribution function of the population is the *empirical (or sample) distribution function* (EDF) of the sample, defined, at any real number x, as the proportion of sample observations which do not exceed x. For a sample of size m, the empirical distribution function will be denoted by $F_m(x)$ and may be defined in terms of the order statistics $X_{(1)} \leq X_{(2)} \cdots \leq X_{(m)}$ by

$$F_m(x) = \begin{cases} 0 & \text{if } x < X_{(1)} \\ j/m & \text{if } X_{(1)} \leq x \leq X_{(j+1)},\ 1 \leq j \leq m \\ 1 & \text{if } x \geq X_{(m)} \end{cases}, \qquad (5)$$

i.e., F_m is the *staircase function*.

To form the test statistics D from the sample distribution functions $F_m(x)$ and $G_n(x)$ we compute their maximum absolute difference over all the values of x,

$$D = \max_x |F_m(x) - G_n(x)|\,. \qquad (6)$$

Graphically, we may interpret this as the maximum vertical displacement between the two sample distribution functions as indicated in Fig. 1.

Testing of the null hypothesis proceeds by comparison of D against critical values D_α which are functions of the confidence level α and the sizes of the samples m, n (Conover, 1967). We may reject the null hypothesis $\mathcal{H}_0$ at the $(1-\alpha)$ confidence level if $D > D_\alpha$. For the case at hand, $m = 9$ and $n = 10$, the upper critical value of the 90% confidence level interval is $D_{0.1} = 5/9$ (Rohlf and Sokal, 1994). Since the maximum difference between the EDFs shown in Fig. 1 is $D = 26/45$, we infer that the null-hypothesis (the two metallicity samples belong to the same distribution) is excluded at the 90% confidence level. Therefore, on the basis of the well-justified assumption that at redshift $z < 0.3$ the host metallicity is a good indicator of the llGRB production rate, we can conclude that the association of llGRBs and the starbursts correlating with Auger data is disfavored by observation.

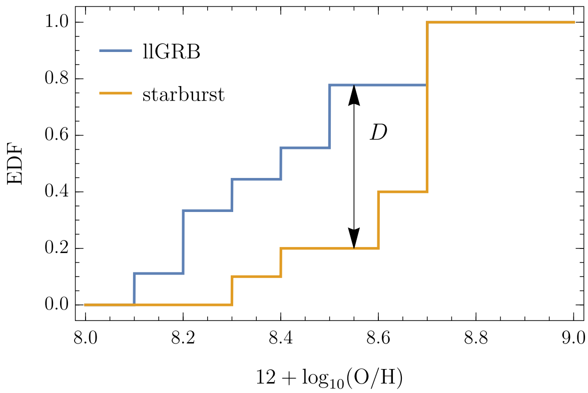

Fig. 1. Vertical displacement between sample distribution functions. (For interpretation of the colors in the figure(s), the reader is referred to the web version of this article.)

3. Conclusion

We have used the metallicity of the llGRB host galaxies as a proxy to investigate whether llGRBs can be the sources of the highest energy cosmic rays whose arrival directions correlate with the celestial positions of nearby starburst galaxies. We have shown that the association of llGRBs and the starbursts correlating with Auger data is excluded at the 90% confidence level. We end with two observations:

- The first one builds upon the estimates in (Pfeffer et al., 2017) and contributes to the debate on the source power requirements. The Telescope Array Collaboration has reported an excess of UHECR events over expectations from a random distribution in a circle of 20° near M82 (Abbasi et al., 2014). The hotspot energy flux in UHECRs with energies $E > E_0 = 5.7 \times 10^{10}$ GeV is estimated to be

$$F_{\rm hs} = \Omega_{20^\circ} \int_{E_0}^{\infty} E \; J_{\rm hs}(E)\, dE \simeq 1.7 \times 10^{-8} \xi_{1.7}\, ({\rm GeV\, cm^2\, s})^{-1}\,, \quad (7)$$

where $\Omega_{20^\circ} \simeq 0.38$ is the hot-spot solid angle and $\xi_{1.7}$ parametrizes the uncertainty in the energy dependence of the specific (number) intensity in the hotspot $J_{\rm hs}(E)$ (Pfeffer et al., 2017). The rms deflection angle for an UHECR of charge Ze is found to be

$$\delta_{\rm rms} \approx 3.6^\circ\; Z\; E_{11}^{-1}\; r_{\rm kpc}^{1/2}\; \lambda_{\rm kpc}^{1/2}\; B_{\mu{\rm G,rms}}\,, \quad (8)$$

where $B_{\mu{\rm G,rms}}$ is the rms strength of the magnetic field in μG, E_{11} is the UHECR energy in units of 10^{11} GeV, $r_{\rm kpc}$ is the distance over which the magnetic fields act in kpc, and $\lambda_{\rm kpc}$ is the magnetic-field coherence length also in units of kpc (He et al., 2016). The scattering in the magnetic field also gives a time spread (Waxman, 1995; Farrar and Piran, 2000), which is given by

$$\tau \simeq 4.1 \left(\frac{r_{\rm kpc} B_{\mu{\rm G}}}{E_{11}}\right)^2 \lambda_{\rm kpc} Z^2 \;{\rm yr} \simeq 4.1 \left(\frac{\delta_{\rm rms}}{3.6^\circ}\right)^2 r_{\rm kpc}\; {\rm yr}\,. \quad (9)$$

Because all the UHECR scattering occurs inside the Galaxy, we have $r_{\rm kpc} \sim 10$ and $\delta_{\rm rms} \sim 20^\circ$, yielding a dispersion of $\tau \sim 10^3$ yr in the UHECR arrival times. For a source at a distance D, the required isotropic equivalent luminosity is $L_{\rm iso} = 4\pi D^2 F_{\rm hs}$ and so the isotropic-equivalent energy implied is $E_{\rm iso} > 10^{51}\; \xi_{1.7}$ erg. It is noteworthy that llGRBs struggle to meet this constraint as they all have $E_{\rm iso} < 10^{50}$ erg (Cano et al., 2017; Stanek et al., 2006). This is also the case for SNe with relativistic outflows but without GRB counterparts, for which the observed isotropic-equivalent energy is on the order of 10^{49} erg (Soderberg et al., 2010; Chakraborti et al., 2015; Margutti et al., 2014).
- We now comment on the possibility that the main hypothesis of our analysis is false; namely, that the host metallicity *is not* a good indicator of the llGRB production rate (see e.g. Kelly et al., 2014; Perley et al., 2016; Palmerio et al., 2019, for a discussion on other considerations that could affect the LGRB production efficiency). In this direction, it is *natural* to envision the most straightforward scenario, in which the llGRB rate is independent of all factors other than the overall rate of star-formation itself. This would imply that a fixed fraction of all newly-formed stars could explode as llGRBs without perception to any of the chemical, physical, or other properties of the galaxy in which those stars formed. From the observational viewpoint, this entails that llGRBs should stochastically sample the locations of cosmic star-formation throughout the volume of the Universe in which they can be observed. The probability that any given galaxy will host a llGRB during some period of time would then be proportional to its star-formation rate. Now, given the ubiquity of llGRBs in this simplistic scenario we can ask ourselves why the correlation of UHECRs with starburst galaxies would be explained by the presence of this *common* phenomenon. Rather there must be some other inherently unique feature(s) of starburst galaxies to account for this correlation. Starburst galaxies represent about 1% of the fraction of galaxies containing star forming galaxies (Bergvall et al., 2016), and the probability of SN explosions is about an order of magnitude larger in starbursts than in normal galaxies, e.g., the SN rate for M82 is about $0.2 - 0.3$ yr^{-1} (Ulvestad and Antonucci, 1994) whereas for the Milky Way is $\sim 3.5 \pm 1.5$ century^{-1} (Dragicevich et al., 1999). Note that these two effects tend to compensate each other, and so if the anisotropy signal reported by the Auger Collaboration originates in llGRBs (within this particular underlying scenario), then when studying the correlation of UHECRs with the nearby matter distribution the statistical significance must increased. However, when all sources beyond 1 Mpc (i.e. effectively taking out the Local Group) from the 2MRS catalog are included as part of the anisotropic signal in the analysis of (Aab et al., 2019) the significance level reduces from 4.5σ to 3.8σ. Altogether, the data yielding the anisotropy signal seem to favor a production mechanism of UHECRs above 38 EeV which is exclusive to starbursts, like Fermi-shock acceleration in starburst superwinds.

Acknowledgments

We thank Michael Unger for useful critique. We also thank our colleagues of the Pierre Auger and POEMMA collaborations for some valuable discussion. This work has been supported by the U.S. National Science Foundation (NSF Grant PHY-1620661) and the National Aeronautics and Space Administration (NASA Grant 80NSSC18K0464). Any opinions, findings, and conclusions or recommendations expressed in this material are those of the authors and do not necessarily reflect the views of the NSF or NASA.

References

Aab, A., et al., Pierre Auger Collaboration, 2018. An Indication of anisotropy in arrival directions of ultra-high-energy cosmic rays through comparison to the flux pattern of extragalactic gamma-ray sources. Astrophys. J. 853 (2), L29. https://doi.org/10.3847/2041-8213/aaa66d. arXiv:1801.06160 [astro-ph.HE].

Aab, A., et al., Pierre Auger Collaboration, 2019. The Pierre Auger Observatory: Contributions to the 36th International Cosmic Ray Conference (ICRC 2019). arXiv:1909.09073 [astro-ph.HE].

Abbasi, R.U., et al., Telescope Array Collaboration, 2014. Indications of intermediate-scale anisotropy of cosmic rays with energy greater than 57 EeV in the Northern sky measured with the surface detector of the Telescope Array experiment. Astrophys. J. 790, L21. https://doi.org/10.1088/2041-8205/790/2/L21. arXiv:1404.5890 [astro-ph.HE].

Ackermann, M., et al., Fermi-LAT Collaboration, 2012. GeV observations of star-forming galaxies with Fermi-LAT. Astrophys. J. 755, 164. https://doi.org/10.1088/0004-637X/755/2/164. arXiv:1206.1346 [astro-ph.HE].

Anchordoqui, L.A., 2018. Acceleration of ultrahigh-energy cosmic rays in starburst superwinds. Phys. Rev. D 97 (6), 063010. https://doi.org/10.1103/PhysRevD.97.063010. arXiv:1801.07170 [astro-ph.HE].

Anchordoqui, L.A., 2019. Ultrahigh-energy cosmic rays. Phys. Rep. 801, 1. https://doi.org/10.1016/j.physrep.2019.01.002. arXiv:1807.09645 [astro-ph.HE].

Anchordoqui, L.A., Soriano, J.F., 2019. Evidence for UHECR origin in starburst galaxies. PoS ICRC 2019 (255). arXiv:1905.13243 [astro-ph.HE].

Anchordoqui, L.A., Romero, G.E., Combi, J.A., 1999. Heavy nuclei at the end of the cosmic ray spectrum? Phys. Rev. D 60, 103001. https://doi.org/10.1103/PhysRevD.60.103001. arXiv:astro-ph/9903145.

Asplund, M., Grevesse, N., Sauval, A.J., Allende Prieto, C., Kiselman, D., 2004. Line formation in solar granulation IV: [O I], OI and OH lines and the photospheric O abundance. Astron. Astrophys. 417, 751. https://doi.org/10.1051/0004-6361:20034328. arXiv:astro-ph/0312290.

Asplund, M., Grevesse, N., Sauval, A.J., Scott, P., 2009. The chemical composition of the Sun. Annu. Rev. Astron. Astrophys. 47, 481. https://doi.org/10.1146/annurev.astro.46.060407.145222. arXiv:0909.0948 [astro-ph.SR].

Bergvall, N., Marquart, T., Way, M.J., Blomqvist, A., Holst, E., Östlin, G., Zackrisson, E., 2016. Local starburst galaxies and their descendants. Astron. Astrophys. 587, A72. https://doi.org/10.1051/0004-6361/201525692. arXiv:1501.06928.

Boncioli, D., Biehl, D., Winter, W., 2019. On the common origin of cosmic rays across the ankle and diffuse neutrinos at the highest energies from low-luminosity Gamma-Ray Bursts. Astrophys. J. 872 (1), 110. https://doi.org/10.3847/1538-4357/aafda7. arXiv:1808.07481 [astro-ph.HE].

Cano, Z., Wang, S.Q., Dai, Z.G., Wu, X.F., 2017. The observer's guide to the gamma-ray burst supernova connection. Adv. Astron. 2017, 8929054. https://doi.org/10.1155/2017/8929054. arXiv:1604.03549 [astro-ph.HE].

Chakraborti, S., et al., 2015. A missing-link in the supernova-GRB connection: the case of SN 2012ap. Astrophys. J. 805 (2), 187. https://doi.org/10.1088/0004-637X/805/2/187. arXiv:1402.6336 [astro-ph.HE].

Chrimes, A., Stanway, E., Levan, A., Davies, L., Angus, C., Greis, S., 2018. Investigating a population of infrared-bright gamma-ray burst host galaxies. Mon. Not. R. Astron. Soc. 478 (1), 2. https://doi.org/10.1093/mnras/sty1043. arXiv:1804.08971 [astro-ph.GA].

Conover, W.J., 1967. A *k*-sample extension of the one-sided two-sample Smirnov test statistic. Ann. Math. Stat. 38, 1726. https://doi.org/10.1214/aoms/1177698606.

Dereli, H., Boër, M., Gendre, B., Amati, L., Dichiara, S., Orange, N.B., 2017. A study of GRBs with low-luminosity afterglows. Astrophys. J. 850 (2), 117. https://doi.org/10.3847/1538-4357/aa947d.

Dopita, M.A., Kewley, L.J., Sutherland, R.S., Nicholls, D.C., 2016. Chemical abundances in high-redshift galaxies: a powerful new emission line diagnostic. Astrophys. Space Sci. 361 (2), 61. https://doi.org/10.1007/s10509-016-2657-8. arXiv:1601.01337 [astro-ph.GA].

Dragicevich, P.M., Blair, D.G., Burman, R.R., 1999. Why are supernovae in our Galaxy so frequent? Mon. Not. R. Astron. Soc. 302, 693. https://doi.org/10.1046/j.1365-8711.1999.02145.x.

Farrar, G.R., Piran, T., 2000. GZK violation: a Tempest in a (magnetic) teapot? Phys. Rev. Lett. 84, 3527. https://doi.org/10.1103/PhysRevLett.84.3527. arXiv:astro-ph/9906431.

Galliano, F., Dwek, E., Chanial, P., 2008. Stellar evolutionary effects on the abundances of PAH and SN-condensed dust in galaxies. Astrophys. J. 672, 214. https://doi.org/10.1086/523621. arXiv:0708.0790 [astro-ph].

He, H.N., Kusenko, A., Nagataki, S., Zhang, B.B., Yang, R.Z., Fan, Y.Z., 2016. Monte Carlo bayesian search for the plausible source of the Telescope Array hotspot. Phys. Rev. D 93, 043011. https://doi.org/10.1103/PhysRevD.93.043011. arXiv:1411.5273 [astro-ph.HE].

Heckman, T.M., 2001. Galactic superwinds at low and high redshift. ASP Conf. Ser. 240, 345. arXiv:astro-ph/0009075.

Hung, D., 2015. Metallicities and temperatures for two metal-rich and two metal-poor galaxies. Undergraduate Research Thesis. The Ohio State University. http://hdl.handle.net/1811/68895.

Izzo, L., et al., 2019. Signatures of a jet cocoon in early spectra of a supernova associated with a γ-ray burst. Nature 565, 324. https://doi.org/10.1038/s41586-018-0826-3. arXiv:1901.05500 [astro-ph.HE].

Jackson, J.M., Paglione, T.A.D., Carlstrom, J.E., Rieu, N.Q., 1995. Submillimeter HCN and HCO+ emission from galaxies. Astrophys. J. 438, 695. https://doi.org/10.1086/175113.

Japelj, J., Vergani, S.D., Salvaterra, R., Renzo, M., Zapartas, E., de Mink, S.E., Kaper, L., Zibetti, S., 2018. Host galaxies of SNe Ic-BL with and without long gamma-ray bursts. Astron. Astrophys. 617, A105. https://doi.org/10.1051/0004-6361/201833209. arXiv:1806.10613 [astro-ph.HE].

Kelly, P.L., Filippenko, A.V., Modjaz, M., Kocevski, D., 2014. The host galaxies of fast-ejecta core-collapse supernovae. Astrophys. J. 789, 23. https://doi.org/10.1088/0004-637X/789/1/23. arXiv:1401.0729 [astro-ph.CO].

Kewley, L.J., Dopita, M.A., 2002. Using strong lines to estimate abundances in extragalactic Hii regions and starburst galaxies. Astrophys. J. Suppl. Ser. 142, 35. https://doi.org/10.1086/341326. arXiv:astro-ph/0206495.

Kewley, L.J., Ellison, S.L., 2008. Metallicity calibrations and the mass-metallicity relation for star-forming galaxies. Astrophys. J. 681, 1183. https://doi.org/10.1086/587500. arXiv:0801.1849 [astro-ph].

Kocevski, D., West, A.A., Modjaz, M., 2009. Modeling the GRB host galaxy mass distribution: are GRBs unbiased tracers of star formation? Astrophys. J. 702, 377. https://doi.org/10.1088/0004-637X/702/1/377. arXiv:0905.1953 [astro-ph.CO].

Kolmogorov, A.N., 1933. Sulla determinazione empirica di una legge di distribuzione. G. Ist. Ital. Attuari 4, 83.

Kouveliotou, C., Meegan, C.A., Fishman, G.J., Bhyat, N.P., Briggs, M.S., Koshut, T.M., Paciesas, W.S., Pendleton, G.N., 1993. Identification of two classes of gamma-ray bursts. Astrophys. J. 413, L101. https://doi.org/10.1086/186969.

Kudritzki, R.P., 2002. Line-driven winds, ionizing fluxes and UV-spectra of hot stars at extremely low metallicity I: very massive O-stars. Astrophys. J. 577, 389. https://doi.org/10.1086/342178. arXiv:astro-ph/0205210.

Kudritzki, R.P., Puls, J., 2000. Winds from hot stars. Annu. Rev. Astron. Astrophys. 38, 613. https://doi.org/10.1146/annurev.astro.38.1.613.

Langer, N., Norman, C.A., 2006. On the collapsar model of long gamma-ray bursts: constraints from cosmic metallicity evolution. Astrophys. J. 638, L63. https://doi.org/10.1086/500363. arXiv:astro-ph/0512271.

Levesque, E.M., Kewley, L.J., Berger, E., Zahid, H.J., 2010. The host galaxies of gamma-ray bursts II: a mass-metallicity relation for long-duration gamma-ray burst host galaxies. Astron. J. 140, 1557. https://doi.org/10.1088/0004-6256/140/5/1557. arXiv:1006.3560 [astro-ph.GA].

Levesque, E.M., Berger, E., Soderberg, A.M., Chornock, R., 2011. Metallicity in the GRB 100316D/SN 2010bh host complex. Astrophys. J. 739, 23. https://doi.org/10.1088/0004-637X/739/1/23. https://doi.org/10.1088/0004-637. arXiv:1104.2865 [astro-ph.HE].

Li, Y., 2017. Understanding progenitors of gamma ray bursts with multi-wavelength properties. PhD Thesis. University of Nevada, Las Vegas. UNLV Theses, Dissertations, Professional Papers, and Capstones, 3087.

Liang, E., Zhang, B., Dai, Z.G., 2007. Low luminosity gamma-ray bursts as a unique population: luminosity function, local rate, and beaming factor. Astrophys. J. 662, 1111. https://doi.org/10.1086/517959. arXiv:astro-ph/0605200.

MacFadyen, A., Woosley, S.E., 1999. Collapsars: gamma-ray bursts and explosions in "failed supernovae". Astrophys. J. 524, 262. https://doi.org/10.1086/307790. arXiv:astro-ph/9810274.

Margutti, R., et al., 2014. Relativistic supernovae have shorter-lived central engines or more extended progenitors: the case of SN 2012ap. Astrophys. J. 797 (2), 107. https://doi.org/10.1088/0004-637X/797/2/107. arXiv:1402.6344 [astro-ph.HE].

Michalowski, M.J., et al., 2018. The second closest gamma-ray burst: sub-luminous GRB 111005A with no supernova in a super-solar metallicity environment. Astron. Astrophys. 616, A169. https://doi.org/10.1051/0004-6361/201629942. arXiv:1610.06928 [astro-ph.HE].

Modjaz, M., Liu, Y.Q., Bianco, F.B., Graur, O., 2016. The spectral SN-GRB connection: systematic spectral comparisons between type Ic supernovae, and broad-lined type Ic supernovae with and without gamma-ray bursts. Astrophys. J. 832 (2), 108. https://doi.org/10.3847/0004-637X/832/2/108. arXiv:1509.07124 [astro-ph.HE].

Moreno-Raya, M.E., Lopez-Sanchez, A.R., Molla, M., Galbany, L., Vilchez, J.M., Carnero, A., 2016. Using the local gas-phase oxygen abundances to explore a metallicity-dependence in SNe Ia luminosities. https://doi.org/10.1093/mnras/stw1706. arXiv:1607.05526 [astro-ph.GA].

Nakar, E., 2015. A unified picture for low-luminosity and long gamma-ray bursts based on the extended progenitor of llGRB 060218/SN 2006aj. Astrophys. J. 807 (2), 172. https://doi.org/10.1088/0004-637X/807/2/172. arXiv:1503.00441 [astro-ph.HE].

Niino, Y., et al., 2017. The redshift selected sample of long gamma-ray burst host galaxies: the overall metallicity distribution at $z < 0.4$. Publ. Astron. Soc. Jpn. 69 (2), 27. https://doi.org/10.1093/pasj/psw133. arXiv:1606.01983 [astro-ph.HE].

Oliva, E., Marconi, A., Moorwood, A.F.M., 1999. Metal abundances and excitation of extranuclear clouds in the Circinus galaxy - a new method for deriving abundances of AGN narrow line clouds. Astron. Astrophys. 342, 87. arXiv:astro-ph/9811177.

Otte, B., Reynolds, R.J., Gallagher III, J.S., Ferguson, A.M.N., 2001. Searching for additional heating - [OII] emission in the diffuse ionized gas of NGC 891, NGC 4631 and NGC 3079. Astrophys. J. 560, 207. https://doi.org/10.1086/322343. arXiv:astro-ph/0106312.

Pagel, B.E.J., Edmunds, M.G., Blackwell, a.D.E., Chun, M.S., Smith, G., 1979. On the composition of H ii regions in southern galaxies I: NGC 300 and 1365. Mon. Not. R. Astron. Soc. 189, 95.

Paglione, T.A.D., Jackson, J.M., Ishizuki, S., 1997. The average properties of the dense molecular gas in galaxies. Astrophys. J. 484, 656. https://doi.org/10.1086/304356.

Palmerio, J.T., et al., 2019. Are long gamma-ray bursts biased tracers of star formation? Clues from the host galaxies of the Swift/BAT6 complete sample of bright LGRBs III: stellar masses, star formation rates, and metallicities at $z > 1$. Astron. Astrophys. 623, A26. https://doi.org/10.1051/0004-6361/201834179. arXiv:1901.02457 [astro-ph.HE].

Perley, D.A., Foley, R.J., Bloom, J.S., Butler, N.R., 2006. GRB 051109B: bright spiral host galaxy at low redshift. GCN Circ., #5387.

Perley, D.A., et al., 2014. The afterglow of GRB 130427A from 1 to 10^{16} GHz. Astrophys. J. 781, 37. https://doi.org/10.1088/0004-637X/781/1/37. arXiv:1307.4401 [astro-ph.HE].

Perley, D.A., Niino, Y., Tanvir, N.R., Vergani, S.D., Fynbo, J.P.U., 2016. Long-duration gamma-ray burst host galaxies in emission and absorption. Space Sci. Rev. 202 (1–4), 111. https://doi.org/10.1007/s11214-016-0237-4. arXiv:1602.00770 [astro-ph.HE].

Pescalli, A., Ghirlanda, G., Salafia, O.S., Ghisellini, G., Nappo, F., Salvaterra, R., 2015. Luminosity function and jet structure of gamma-ray burst. Mon. Not. R. Astron. Soc. 447 (2), 1911. https://doi.org/10.1093/mnras/stu2482. arXiv:1409.1213 [astro-ph.HE].

Pettini, M., Pagel, B.E.J., 2004. [Oii] / [Nii] as an abundance indicator at high redshift. Mon. Not. R. Astron. Soc. 348, L59. https://doi.org/10.1111/j.1365-2966.2004.07591.x. arXiv:astro-ph/0401128.

Pfeffer, D.N., Kovetz, E.D., Kamionkowski, M., 2017. Ultrahigh-energy cosmic ray hotspots from tidal disruption events. Mon. Not. R. Astron. Soc. 466 (3), 2922. https://doi.org/10.1093/mnras/stw3337. arXiv:1512.04959 [astro-ph.HE].

Pilyugin, L.S., Vilchez, J.M., Contini, T., 2004. Oxygen and nitrogen abundances in nearby galaxies: correlations between oxygen abundance and macroscopic properties. Astron. Astrophys. 425, 849. https://doi.org/10.1051/0004-6361:20034522. arXiv:astro-ph/0407014.

Rohlf, F.J., Sokal, R.R., 1994. Statistical Tables, third ed. W. H. Freeman and Company. ISBN 9780716724124.

Samuelsson, F., Bégué, D., Ryde, F., Pe'er, A., 2019. The limited contribution of low- and high-luminosity gamma-ray bursts to ultrahigh-energy cosmic rays. Astrophys. J. 876 (2), 93. https://doi.org/10.3847/1538-4357/ab153c. arXiv:1810.06579 [astro-ph.HE].

Smirnov, N.V., 1933. Estimate of deviation between empirical distribution functions in two independent samples Bulletin Moscow University 2, 3.

Soderberg, A.M., et al., 2010. Discovery of a relativistic supernova without a gamma-ray trigger. Nature 463, 513. https://doi.org/10.1038/nature08714. arXiv:0908.2817 [astro-ph.HE].

Stanek, K.Z., et al., 2006. Protecting life in the milky way: metals keep the grbs away. Acta Astron. 56, 333. arXiv:astro-ph/0604113.

Stanghellini, L., Magrini, L., Casasola, V., 2015. Gas-phase oxygen abundances and radial metallicity gradients in the two nearby spiral galaxies NGC7793 and NGC4945. Astrophys. J. 812, 39. https://doi.org/10.1088/0004-637X/812/1/39. arXiv:1508.02754.

Stanway, E.R., Levan, A.J., Tanvir, N.R., Wiersema, K., van der Horst, A., Mundell, C.G., Guidorzi, C., 2015. GRB 080517: a local, low-luminosity gamma-ray burst in a dusty galaxy at $z = 0.09$. Mon. Not. R. Astron. Soc. 446 (4), 3911. https://doi.org/10.1093/mnras/stu2286. arXiv:1409.5791 [astro-ph.GA].

Tanga, M., Krühler, T., Schady, P., Klose, S., Graham, J.F., Greiner, J., Kann, D.A., Nardini, M., 2018. The environment of the SN-less GRB 111005A at $z = 0.0133$. Astron. Astrophys. 615, A136. https://doi.org/10.1051/0004-6361/201731799. arXiv:1708.06270 [astro-ph.GA].

Tendulkar, S.P., et al., 2017. The host galaxy and redshift of the repeating fast radio burst FRB 121102. Astrophys. J. 834 (2), L7. https://doi.org/10.3847/2041-8213/834/2/L7. arXiv:1701.01100 [astro-ph.HE].

Thöne, C.C., et al., 2008. Spatially resolved properties of the GRB 060505 host: implications for the nature of the progenitor. Astrophys. J. 676, 1151. https://doi.org/10.1086/528943. astro-ph/0703407 [ASTRO-PH].

Thöne, C.C., et al., 2019. Outflows from dwarf starbursts are ubiquitous: kinematics of $z < 0.3$ GRB-SN hosts resolved with FLAMES. arXiv:1904.05935 [astro-ph.HE].

Tremonti, C.A., et al., 2004. The origin of the mass-metallicity relation: insights from 53,000 star-forming galaxies in the SDSS. Astrophys. J. 613, 898. https://doi.org/10.1086/423264. arXiv:astro-ph/0405537.

Trenti, M., Perna, R., Jimenez, R., 2015. The luminosity and stellar mass functions of GRB host galaxies: insight into the metallicity bias. Astrophys. J. 802 (2), 103. https://doi.org/10.1088/0004-637X/802/2/103. arXiv:1406.1503 [astro-ph.GA].

Ulvestad, J.S., Antonucci, R.R.J., 1994. Do the compact radio sources in NGC 253 and M82 fade over time? Astrophys. J. 424, L32. https://doi.org/10.1086/187267.

Vink, J.S., de Koter, A., 2005. On the metallicity dependence of Wolf-Rayet winds. Astron. Astrophys. 442, 587. https://doi.org/10.1051/0004-6361:20052862.

Virgili, F., Liang, E., Zhang, B., 2009. Low-luminosity gamma-ray bursts as a distinct GRB population: a Monte Carlo analysis. Mon. Not. R. Astron. Soc. 392, 91. https://doi.org/10.1111/j.1365-2966.2008.14063.x. arXiv:0801.4751 [astro-ph].

Waxman, E., 1995. Cosmological gamma-ray bursts and the highest energy cosmic rays. Phys. Rev. Lett. 75, 386. https://doi.org/10.1103/PhysRevLett.75.386. arXiv:astro-ph/9505082.

Woosley, S., Heger, A., 2006. The progenitor stars of gamma-ray bursts. Astrophys. J. 637, 914. https://doi.org/10.1086/498500. arXiv:astro-ph/0508175.

Woosley, S.E., Bloom, J.S., 2006. The supernova gamma-ray burst connection. Annu. Rev. Astron. Astrophys. 44, 507. https://doi.org/10.1146/annurev.astro.43.072103.150558. arXiv:astro-ph/0609142.

Yoon, S.C., Dierks, A., Langer, N., 2012. Evolution of massive population III stars with rotation and magnetic fields. Astron. Astrophys. 542, A113. https://doi.org/10.1051/0004-6361/201117769. arXiv:1201.2364 [astro-ph.SR].

Zaritsky, D., Kennicutt, R.C., Huchra, J.P., 1994. Hii regions and the abundance properties of spiral galaxies. Astrophys. J. 420, 87. https://doi.org/10.1086/173544.

Zhang, B.T., Murase, K., 2018. Ultrahigh-energy cosmic-ray nuclei and neutrinos from engine-driven supernovae. arXiv:1812.10289 [astro-ph.HE].

Zhang, B.T., Murase, K., Kimura, S.S., Horiuchi, S., Mészáros, P., 2018. Low-luminosity gamma-ray bursts as the sources of ultrahigh-energy cosmic ray nuclei. Phys. Rev. D 97 (8), 083010. https://doi.org/10.1103/PhysRevD.97.083010. arXiv:1712.09984 [astro-ph.HE].